# Numerical Study of Transonic Axial Flow Rotating Cascade Aerodynamics – Part 1: 2D Case

Irina Carmen ANDREI*

*Corresponding author
INCAS – National Institute for Aerospace Research "Elie Carafoli"
B-dul Iuliu Maniu 220, Bucharest 061126, Romania
andrei.irina@incas.ro, icandrei28178@gmail.com

DOI: 10.13111/2066-8201.2014.6.2.1

***Abstract**: The purpose of this paper is to present a 2D study regarding the numerical simulation of flow within a transonic highly-loaded rotating cascade from an axial compressor. In order to describe an intricate flow pattern of a complex geometry and given specific conditions of cascade's loading and operation, an appropriate accurate flow model is a must. For such purpose, the Navier-Stokes equations system was used as flow model; from the computational point of view, the mathematical support is completed by a turbulence model. A numerical comparison has been performed for different turbulence models (e.g. KE, KO, Reynolds Stress and Spallart-Allmaras models). The convergence history was monitored in order to focus on the numerical accuracy. The force vector has been reported in order to express the aerodynamics of flow within the rotating cascade at the running regime, in terms of Lift and Drag. The numerical results, expressed by plots of the most relevant flow parameters, have been compared. It comes out that the selecting of complex flow models and appropriate turbulence models, in conjunction with CFD techniques, allows to obtain the best computational accuracy of the numerical results. This paper aims to carry on a 2D study and a prospective 3D will be intended for the same architecture.*

***Key Words**: aerodynamics of flow, axial cascades/ axial compressor, transonic, numerical simulation, Navier-Stokes equations, turbulence models, flow solver.*

## I. INTRODUCTION

Modern engines features are continuously setting new standards of performance and reliability while satisfying the environmental friendly demands, i.e. tough limits for aircraft noise and emissions level.

Advanced aerodynamics together with composite fans are assets of the propulsion technology that produce a quieter engine. The sound level of the jet engines can be reduced by the new design of the larger fan blades; as larger fans turn slower than the smaller ones, then the velocity of air is reduced and therefore the noise is lowered. But larger fans involve larger diameters and the velocity at blade tip can be transonic up to supersonic unless the rotational speed diminishes. The engine thrust can be increased with larger compressor pressure ratios and more stages. By the design of highly loaded cascades, the number of the compressor stages is reduced, as well as the parts weight. The fewer the compressor stages, the fewer parts and fewer costs.

As it comes up from the real running conditions, the aerodynamics of flow within the fan and the core engine is unsteady, the viscosity and the 3D (rather than the 2D) specificity must be taken into account. A thorough investigation of the flow is achieved by experiment, theory and CFD.

The computational analysis of flow proves to be a reliable tool for the design, as it allows exposing unsteady flow data in complex geometry of rotating configurations, which sometimes prove to be difficult to access instrumentally.

Obtaining accurate computations represents a heavy task for solving complex flow problems and it is hampered by the computational resources (namely the CPU power and storage capacity).

On the other hand, aiming for the computational accuracy and results reliability, when using an appropriate CFD code such as the FLUENT, it is important to set properly the code's parameters.

It comes out that for an adequate management of the code settings required for a 3D computation, one should check up the settings within 2D computations by using several turbulence models attached to the flow model. Following the specificity of the real flow (i.e. viscous, compressible) the Navier-Stokes equations system represents the best option for the flow model.

Focusing the convergence of the solution and the accuracy of the 2D computations, one can select the turbulence model TM and then set appropriately the code's parameters for the 3D computation of flow.

An overview of the turbulence models that are being used in 3D turbomachinery CFD can be found in the study of Gerolymos, Neubauer, Sharma and Vallet, [16], as pointed out in Table 1.

Table 1 – Turbulence models used in 3D turbomachinery CFD, [16]

| Authors | Date | Closure | Model | Space | Time |
|---|---|---|---|---|---|
| Hah | 1986 | 2-eqns. | ARSM | $O(\Delta x^2)$ upwind | Implicit |
| Dawes | 1987 | 0-eqns. | ML | $O(\Delta x^2)$ centered | Implicit PB |
| Hah | 1988 | 2-eqns. | $k$-$\varepsilon$ | $O(\Delta x^2)$ upwind | Implicit |
| Adamczyk et al. | 1990 | 0-eqns. | ML | $O(\Delta x^2)$ centered | RK+IRS |
| Chima | 1990 | 0-eqns. | ML | $O(\Delta x^2)$ centered | RK+IRS |
| Laksminarayana et al. | 1992 | 2-eqns. | $k$-$\varepsilon$ | $O(\Delta x^2)$ centered | RK |
| Denton | 1992 | 0-eqns. | ML | $O(\Delta x^2)$ centered | Explicit+ Multigrid |
| Dawes | 1992 | 2-eqns. | $k$-$\varepsilon$ | $O(\Delta x^2)$ centered, unstructured grid | RK+IRS |
| Hirsch et al. | 1993 | 0-eqns. | ML | $O(\Delta x^2)$ centered | RK+IRS |
| Amone | 1993 | 0-eqns. | ML | $O(\Delta x^2)$ centered | RK+IRS+Multigrid |
| Turner and Jennions | 1993 | 2-eqns. | $k$-$\varepsilon$ WF | $O(\Delta x^2)$ centered | RK |
| Vogel et al. | 1997 | 2-eqns. | $k$-$\omega_T$ | $O(\Delta x^2)$ centered | RK |
| Ameri et al. | 1998 | 2-eqns. | $k$-$\omega_T$ | $O(\Delta x^2)$ centered | RK+IRS+Multigrid |
| Furukawa et al. | 1998 | 0-eqns. | ML | $O(\Delta x^3)$ upwind | Implicit |
| Rhie et al. | 1998 | 2-eqns. | $k$-$\varepsilon$ | $O(\Delta x^2)$ centered | Implicit PB |
| Gerolymos and Vallet | 1998 | 2-eqns. | $k$-$\varepsilon$ | $O(\Delta x^3)$ upwind | Implicit |
| Arima et al. | 1999 | 2-eqns. | $k$-$\varepsilon$ | $O(\Delta x^3)$ TVD | Implicit |

| | | | | | |
|---|---|---|---|---|---|
| Fritsch et al. | 1999 | 2-eqns. | *k-ε* | $O(\Delta x^2)$ centered | RK+IRS |
| Sayma et al. | 2000 | 1-eqns. | 1-eqn. | $O(\Delta x^2)$ centered | Implicit |
| Launder et al.<br>Speziale et al. | 1975-1991 | 7-eqns. | RSM | $O(\Delta x^3)$ upwind | Implicit |
| Menter | 1993 | 2-eqns. | SST *k-ω* | $O(\Delta x^2)$ centered | Implicit |

The significance of the abbreviations in Table 1 is as follows: WF = wall functions, IRS = implicit residual smoothing, PB = pressure based, RK = Runge – Kutta, ML = mixing length, ARSM = algebraic Reynolds stress model, RSM = Reynolds stress model, SST = Shear Stress Transport.

According to Gerolymos, Neubauer, Sharma and Vallet, [16], the ***Reynolds Stress*** model **RSM** gives better results than the models based on mixing length and is not influenced by the topology of the grid. The RSM is less grid sensitive than the ***k-ε*** model. On the other hand, the ***k-ε*** model applied on a fine grid, gives accurate results as long as the boundary layer does not separate.

The convergence rate of the RSM decays with about 30 % with respect to the ***k-ε*** model when it captures a separation, [16]. For the reason of economy (i.e. fewer iterations required up to getting the convergence) the ***k-ε*** model is preferred by many authors, e.g. Celestina, [15], [17], Hathaway, [13].

The ***Spalart-Allmaras*** model can be also selected, as it consists of one equation and gives good results for flows with larger Reynolds numbers, according to Clark & Hall, [21], and Imregun, [19].

Within this paper several 2D flow computations have been carried out with the CFD code FLUENT, with the turbulence being described by 4 models, i.e.: (TM**1**) the one equation ***Spalart-Allmaras*** model, (TM**2**) the two equations ***k-ε*** model, (TM**3**) the three equations ***k-ω*** model and (TM**4**) the five equations ***Reynolds Stress*** model **RSM**.

All the computations have been performed for a representative blade spanwise section, i.e. the **mid-span**, located at half distance between the hub and tip blade.

## II. DESCRIPTION OF THE STUDY CASE

### II.1 Briefing on geometry and aerodynamics

The **study case** is represented by a transonic highly loaded rotor cascade of the first stage of a 7 staged axial compressor, [1].

The flow is said [7] to be transonic in the rotating blades if the relative Mach number at the inlet is larger than 1, i.e. $M_w > 1$. At the design point, the following data are specified in [1], [10]: *pressure ratio* $\pi_c^* = 9$, *speed nc=5500 [rpm]*, *rotation* $\Omega = 576 \cdot [s^{-1}]$, *specific work on compression* $l_c^* = 310 \cdot [kJ/kg]$ for the 7 staged axial flow compressor and $l_{tr.1}^* = 34.2 \cdot [kJ/kg]$ for the first stage.

Also, we find *the stage pressure ratio* $\pi_{c\,tr.1}^* = 1.4243$, *rotor pressure ratio* $\pi_{R.1}^* = 1.4312$, *stator pressure recovery* $\sigma_{S.1}^* = 0.9952$. The flow path is convergent, designed with a constant *radius* at rotor blade tip $R_V$*=635 [mm]*.

Fully design details about the study case are given in refs. [1], [9,10] and [27]; the aerodynamics of the compressor was computed with the *Fully Radial Equilibrium Theory*, by Creveling & Carmody, [10].

Back up engineering, i.e. the radial design of the blade was carried on by the author, using NACA 65 series airfoils. A summary of cascade design parameters is presented in Table 2, for the mid-span blade section <**M**> that has been considered for the **2D** flow **analysis**.

Table 2 – Summary of cascade design parameters

| Parameter | Blade span-wise Section: **M** = *mid-span* |
|---|---|
| Airfoil | NACA 652010 |
| Radii ***R*** [*mm*] at inlet / exit | 476,5 / 506.5 |
| Chord ***b*** [*mm*] | 62 |
| Pitch ***t*** [*mm*] | 42 |
| Relative pitch | 0.683 |
| Camber $\theta$ [°] | 14,665 |
| Stagger $\beta_f$ [°] | 41,901 |
| Reynolds [1] number | $> 1.24 \cdot 10^6$ |
| Inlet flow angle $\beta_1$ [°] | 34,084 |
| Exit flow angle $\beta_2$ [°] | 43,861 |
| Deviation $\Delta\beta$ [°] | 9,777 |
| Diffusion factor $D_R$ | 0,3544 |
| Inlet Mach $M_C$_1 | 0,605 |
| Exit Mach $M_C$ _2 | 0,6205 |
| Inlet Mach $M_W$ _1 | 1,08 |
| Exit Mach $M_W$ _2 | 0,762 |
| Total pressure [*bar*] at inlet / exit | 1.01352 / 1.44376 |
| Total temperature [*K*] at inlet / exit | 289 / 323 |
| Stagnation pressure [*bar*] at inlet / exit | 0.05459 / 1.15556 |
| Stagnation temperature [*K*] at inlet / exit | 269 / 303 |
| Axial velocity [*m/s*] at inlet / exit | 196 /179.40 |
| Radial velocity [*m/s*] at inlet / exit | 33.74 / 36.78 |
| Tangential velocity [*m/s*] at inlet / exit | 0 / 113.06 |
| *N.B. Mach number of absolute flow is referred by $M_C$, while Mach number in relative frame is referred by $M_W$; index _1 is applied for the cascade's inlet section and index _2 stands for the ecascade's exit section.* | |

The first stage at mid-span features a 0.907 *reaction degree*, a 0.6063 *flow coefficient* (1) and a 0.3585 *blade loading coefficient* (2).

$$\overline{C}_a = \frac{C_a}{u} \tag{1}$$

$$\bar{l}_u = \frac{l_{treapta}}{u^2} \tag{2}$$

## III. COMPUTATIONAL DETAILS

### III.1 Computational domain and grid

The H-type grid that was built over the computational domain with the GAMBIT code, has 13028 nodes (with 2 x 81 nodes on each: *suction side* SS and *pressure side* PS, and 81 nodes along the blade-to-blade direction), as shown in Fig. 1.

[1] Reynolds number was computed with the relative velocity at cascade inlet and chord.

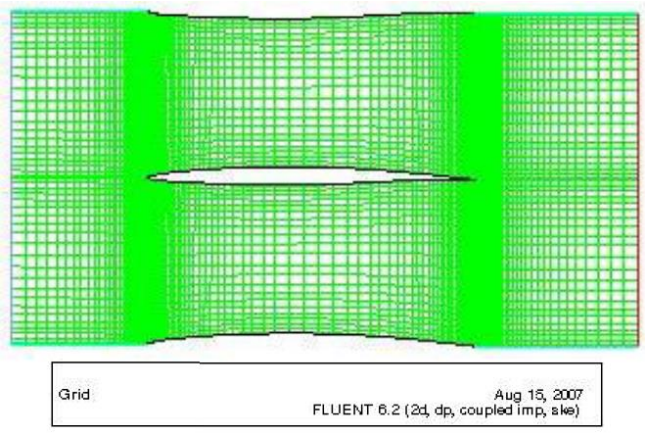


Fig. 1 – Grid at mid-span rotor blade section

The nodes are not equally spaced, but concentrated around the *leading edge* LE, the *trailing edge* TE and in the vicinity of the *suction side* SS and *pressure side* PS.

### III.2 Flow and turbulence models

The Navier-Stokes equations system was used to model the flow. As regards the turbulence models the following have been considered: (TM**1**) the one equation ***Spalart-Allmaras*** model, (TM**2**) the two equations standard ***k-ε*** model, (TM**3**) the three equations standard ***k-ω*** model and (TM**4**) the five equations ***Reynolds Stress*** model **RSM**.

### III.3 A briefing of the FLUENT setting options

*Coupled* **solver**/ *implicit* **formulation**/ *2D* **space**/ *steady* **time**/ *absolute* **velocity formulation**/ *cell based* **gradient option**/ *superficial velocity* **porous formulation**. The implicit coupled solver can be run at larger CFL numbers, without going into divergence.

Boundary conditions were set in accordance with the input data. For the inlet boundary the pressure – inlet type conditions were set; the values of the pressure and static temperature allow to check the specified axial velocity of 196 [m/s]. Similar options have been set on the exit boundary, i.e. *pressure-outlet* type, in compliance with the data available from design and general aerodynamics, see also Table 2.

The computations have been carried on for each turbulence model, considering the rotation speed ***u*** *[m/s]* ranging from 0 up to 275 (i.e. the real case).

Table 3 describes the iterations to go until convergence is reached, for each of the 4 turbulence models considered. The option for solution controls were: *Courant* number = *2* and first order upwind schemes.

Table 3 – Number of iterations till convergence reached

| **Turbulence Model** | Rotation speed $\boldsymbol{u}\ [m/s]$ | | | | | |
|---|---|---|---|---|---|---|
| | 0 | 100 | 150 | 200 | 250 | **275** |
| (TM1) ***Spalart-Allmaras*** | 3105 | 3134 | 3144 | 3151 | 3157 | **3160** |
| (TM2) ***k-ε*** | 2850 | 2878 | 2895 | 2905 | 2917 | **2923** |
| (TM3) ***k-ω*** | 5097 | 5117 | 5121 | 5120 | 5117 | **5115** |
| (TM4) ***RSM*** | 3163 | 3214 | 3241 | 3265 | 3294 | **3308** |

## IV. RESULTS

The most significant computed parameters have been presented comparatively with regard to the 4 considered turbulence models. The contours of relative Mach number have been shown in Fig. 2 (*filled contours*) and Fig. 6 (*iso*-Mach *lines*), since the relative velocity is a significant parameter for the rotating cascades. The contours of static pressure have been presented in Fig. 3 and the contours of static temperature, in Fig. 4.

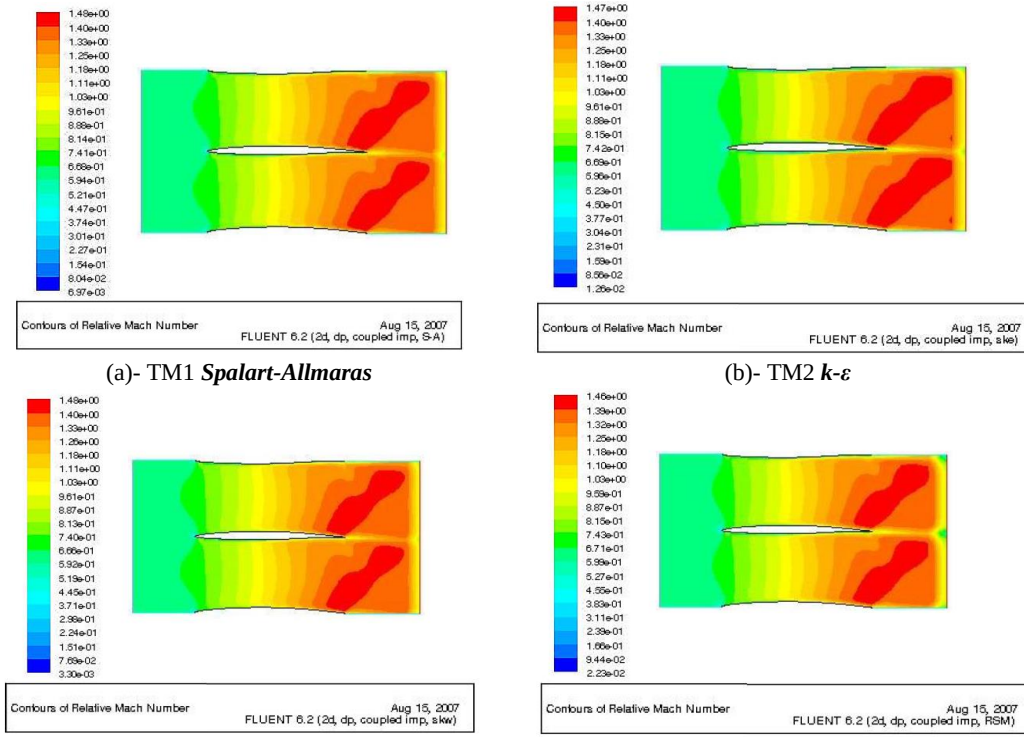


(a)- TM1 ***Spalart-Allmaras*** (b)- TM2 ***k-ε***

(c)- TM3 ***k-ω*** (d)- TM4 ***RSM***

Fig. 2 – Contours of relative Mach number

The pressure coefficient on both *suction side* and *pressure side* (i.e. on the airfoil surface) has been depicted in Fig.5; it comes out that from this point of view, the 4 turbulence models allow to get (almost) the same results when speaking about the pressure coefficient on the airfoil surface.

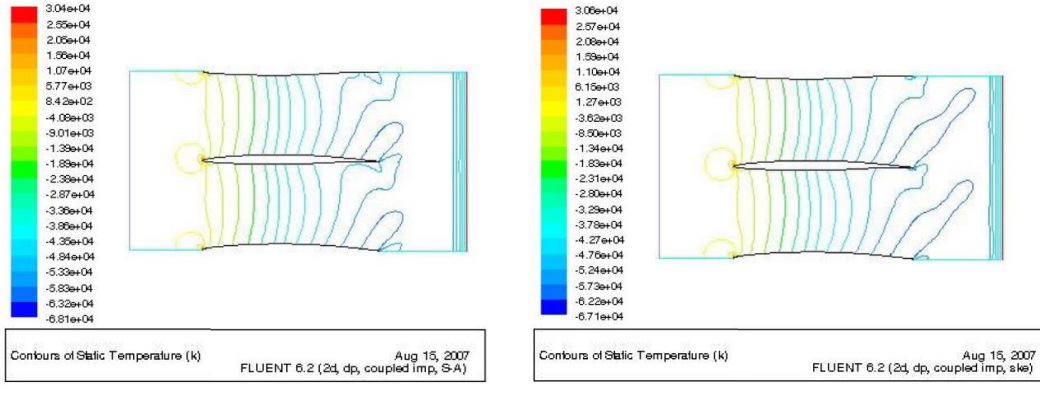


(a)- TM1 ***Spalart-Allmaras*** (b)- TM2 ***k-ε***

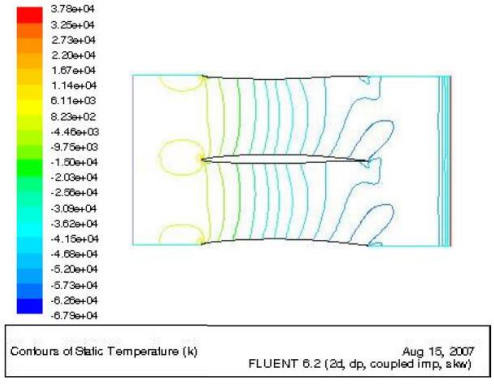


(c)- TM3 ***k-ω***

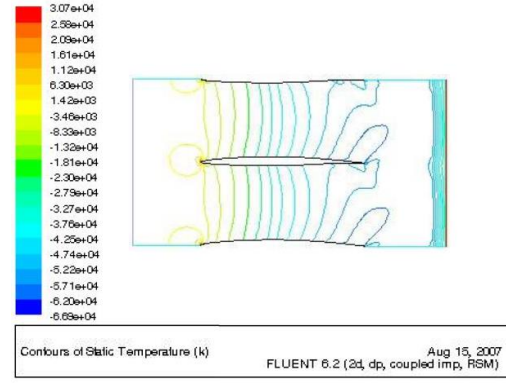


(d)- TM4 ***RSM***

Fig. 3 – Contours of static pressure

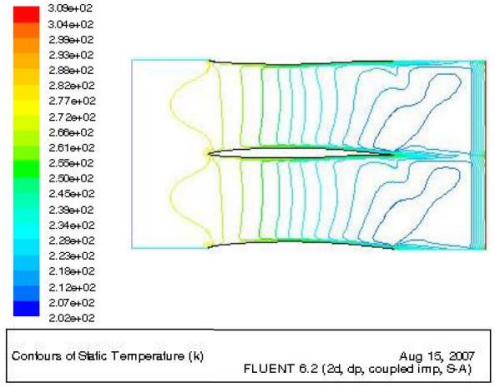


(a)- TM1 ***Spalart-Allmaras***

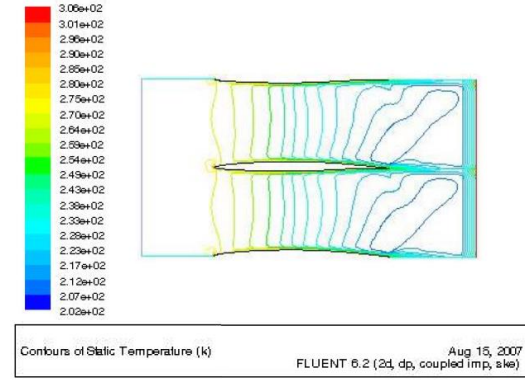


(b)- TM2 ***k-ε***

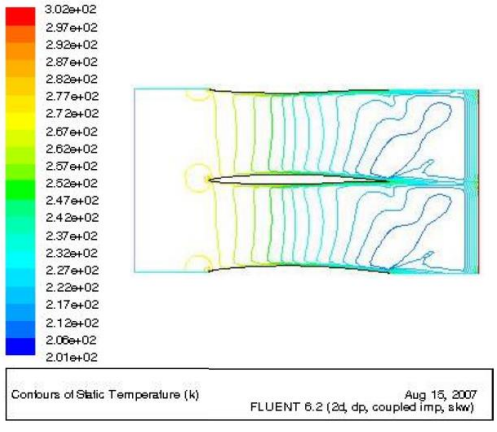


(c)- TM3 ***k-ω***

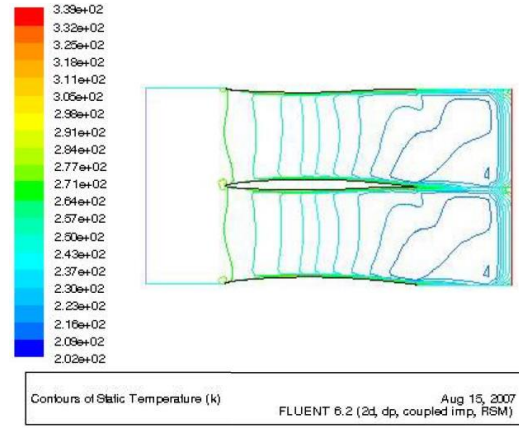


(d)- TM4 ***RSM***

Fig. 4 – Contours of static temperature

The results of the computations carried on with each turbulence model TM are similar but not identical, as one can easily notice in Figs. 3, 4 and 6, as well as in Tables 4 and 5.

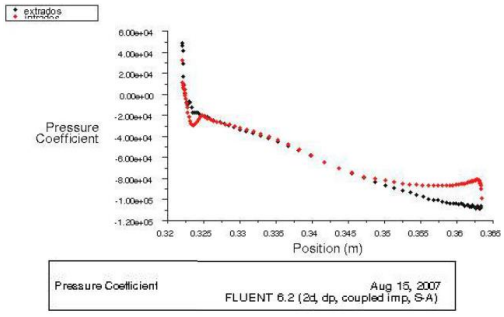


(a)- TM1 ***Spalart-Allmaras***

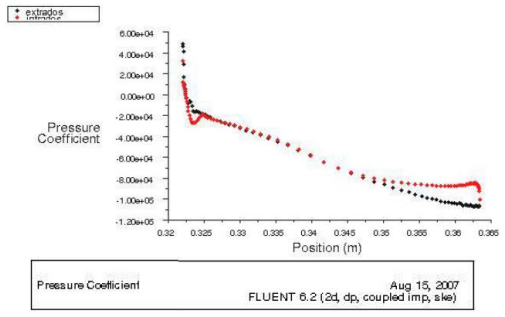


(b)- TM2 ***k-ε***

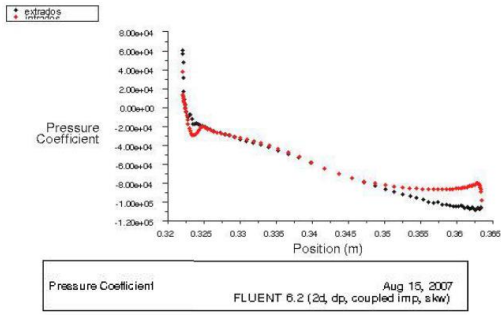


(c)- TM3 ***k-ω***

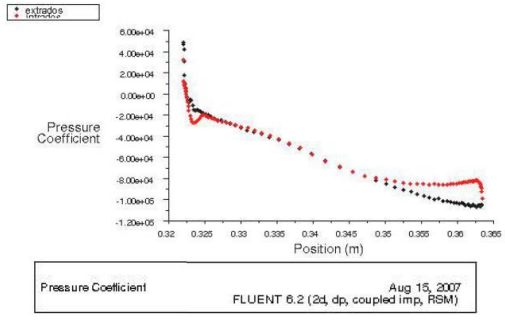


(d)- TM4 ***RSM***

Fig. 5 – Pressure coefficient on airfoil

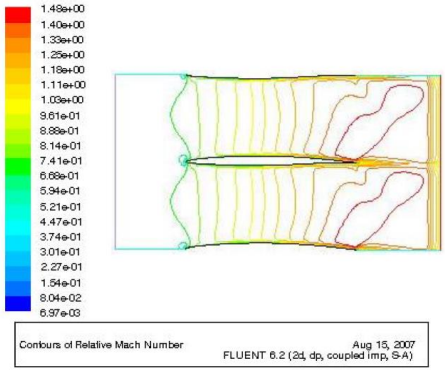


(a)- TM1 ***Spalart-Allmaras***

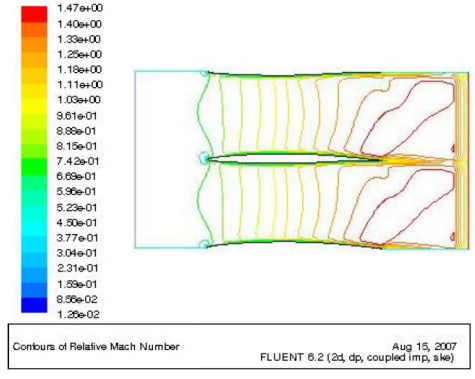


(b)- TM2 ***k-ε***

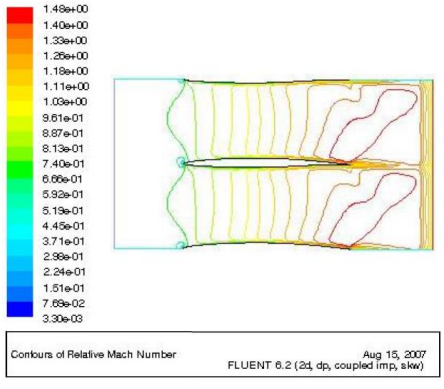


(c)- TM3 ***k-ω***

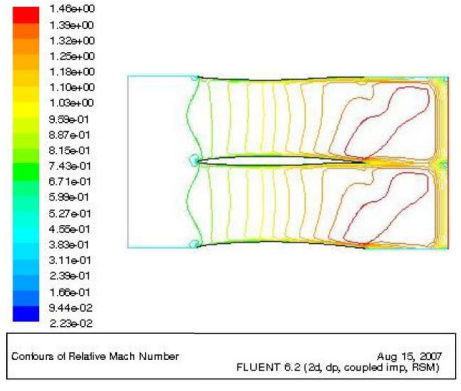


(d)- TM4 ***RSM***

Fig. 6 – Contours of relative Mach number (*iso-Mach* lines)

The contribution of the terms issued due to the pressure and viscosity was considered for the computation of *Lift* and *Drag* forces, as well as of the aerodynamic moment. The influence of the pressure force and viscous force on the forces developed on the airfoil (i.e. *Lift* & *Drag*) has been reported in Table 4 for *Lift* and in Table5 for *Drag*.

For each case, the balance of flows has been monitored whilst crossing the computational domain, which is presented in Fig. 1.

Table 4 – Report on Force vector (0,1,0) → Lift

| **Turbulence Model** | *Zone/ Airfoil side* | Pressure force n | Viscous force n | Total force n | Pressure coefficient | Viscous coefficient | Total coefficient |
|---|---|---|---|---|---|---|---|
| (TM1) ***Spalart-Allmaras*** | *SS* | 1623.44 | -0.128 | 1623.31 | 2650.51 | -0.208 | 2650.30 |
| | *PS* | -1522.8 | -0.207 | -1523.06 | -2486.29 | -0.337 | -2486.62 |
| | net | 100.59 | -0.334 | 100.25 | 164.22 | -0.545 | 163.68 |
| (TM2) ***k-ε*** | *SS* | 1637.98 | -0.1087 | 1637.88 | 2674.26 | -0.177 | 2674.08 |
| | *PS* | -1527.99 | -0.1102 | -1578.11 | -2494.69 | -0.180 | -2494.81 |
| | net | 109.99 | -0.2189 | 109.77 | 179.57 | -0.357 | 179.21 |
| (TM3) ***k-ω*** | *SS* | 1634.20 | -0.1788 | 1634.02 | 2668.08 | -0.292 | 2667.79 |
| | *PS* | -1524.56 | -0.0912 | -1524.65 | -2489.08 | -0.149 | -2489.23 |
| | net | 109.64 | -0.2700 | 109.37 | 179.00 | -0.441 | 178.56 |
| (TM4) ***RSM*** | *SS* | 1599.08 | -0.2715 | 1598.80 | 2610.74 | -0.443 | 2610.29 |
| | *PS* | -1501.48 | -0.0792 | -1501.56 | -2451.40 | -0.129 | -2451.53 |
| | net | 97.59 | -0.3506 | 97.24 | 159.34 | -0.572 | 158.76 |

Table 5 – Report on Force vector (1,0,0) → Drag

| **Turbulence Model** | *Zone/ Airfoil side* | Pressure force n | Viscous force n | Total force n | Pressure coefficient | Viscous coefficient | Total coefficient |
|---|---|---|---|---|---|---|---|
| (TM1) ***Spalart-Allmaras*** | *SS* | 84.0 | 13.33 | 97.33 | 137.15 | 21.76 | 158.91 |
| | *PS* | 20.7 | 11.38 | 32.09 | 33.81 | 18.59 | 52.39 |
| | net | 104.7 | 24.71 | 129.43 | 170.96 | 40.35 | 214.30 |
| (TM2) ***k-ε*** | *SS* | 84.12 | 8.49 | 92.62 | 137.35 | 13.87 | 151.21 |
| | *PS* | 20.42 | 8.19 | 28.62 | 33.35 | 13.37 | 46.72 |
| | net | 104.54 | 16.68 | 121.24 | 170.70 | 27.24 | 197.93 |
| (TM3) ***k-ω*** | *SS* | 83.5 | 9.05 | 92.55 | 136.33 | 14.78 | 151.11 |
| | *PS* | 20.36 | 8.45 | 28.81 | 33.24 | 13.79 | 47.03 |
| | net | 103.86 | 17.50 | 121.36 | 169.57 | 28.57 | 198.14 |
| (TM4) ***RSM*** | *SS* | 83.52 | 14.26 | 97.78 | 136.36 | 23.28 | 159.64 |
| | *PS* | 20.48 | 13.55 | 34.03 | 33.44 | 22.13 | 55.57 |
| | net | 104.00 | 27.81 | 131.81 | 169.80 | 45.41 | 215.21 |

## V. CONCLUSIONS

For the rotating cascade at the running regime (i.e. the rotation speed $u=275$ [*m/s*]), the convergence was achieved after a different number of iterations, as pointed out in Table 6. The appropriate turbulence model can be selected (when experimental data is not available) such that the best computational accuracy should be obtained. By monitoring the residuals history, one can get the information on the number of iterations till the convergence is attained. Minimizing the residuals with the least number of iterations (which mean less CPU time) indicates the adequate selection of the turbulence model.

In this case, the (TM2) ***k-ε*** is the most convenient, as it requires the least number of iterations. Not very far as regards the rate of convergence are the (TM1) ***Spalart-Allmaras*** and (TM3) **RSM** models, as shown in Table 6.

Table 6 – Summary of convergence rates

| **Turbulence Model** | **Iterations** | **Ratio of convergence rates [%]** | | | |
|---|---|---|---|---|---|
| | | ***k-ε*** | ***Spalart-Allmaras*** | ***RSM*** | ***k-ω*** |
| (TM2) ***k-ε*** | **2923** | --- | 10.8 | 11.3 | 17.5 |
| (TM1) ***Spalart-Allmaras*** | **3160** | 10.8 | --- | 10.5 | 16.2 |
| (TM4) ***RSM*** | **3308** | 11.3 | 10.5 | --- | 15.5 |
| (TM3) ***k-ω*** | **5115** | 17.5 | 16.2 | 15.5 | --- |

The purpose of carrying a 2D computation is to allow for a proper selection of the CFD code (e.g. FLUENT) parameters for running the 3D case of a specified problem.

The **outlook** is to do 3D computations, for both un-swept and swept blades, since by the use of sweep to jet engines design proves to be an optimization method. The effects of the blade sweep are the lowering from the supersonic to the transonic and/ or subsonic level of the flow velocity at the tip blade, and therefore the diminishing in noise level, as well as the blade loss that can be cut or significantly reduced.

The experience achieved within the present 2D CFD study, in conjunction with the survey of axial flow compressors and fans with swept blades purposed for jet engines, [1, 10-24, 26-29], as well as the building of a customized swept blade constructions data base, will facilitate the investigation of the optimized construction with the aid of 3D CFD study. The use of sweep together with advanced aerodynamics blade design allows creating highly efficient construction of modern jet engine parts.

## REFERENCES

[1] I. C. Andrei, *Researches with Regard to Studying the Flow Through Axial Compressor Cascades and Potential Means in Purpose to Performance Improvement, with Applications to the Jet Engines*, Ph. D. Thesis, University „POLITEHNICA" of Bucharest, 2007, Central Library index: 043/3219, 533.6(043.2) 621.51.001, 5(043.2) 621.45(043.2) B-UP 1.

[2] J. H. Ferziger, M. Perić, *Computational Methods for Fluid Dynamics*, 3rd Edition, Springer Verlag, 2002.

[3] K. Srinivas, C. A. J. Fletcher, *Computational Techniques for Fluid Dynamics*, Volume 1, Fundamental and General Techniques, Second Edition, Springer Series in Computational Physics, Springer Verlag, 1991, ISSN 0172-5726, ISBN 3-540-53058-4.

[4] David. C. Wilcox, Turbulence Modeling for CFD, 3rd edition, DCW Industries, Inc., La Canada, California, 2006, ISBN 978-1-928729-08-2

[5] T. J. Chung, *Computational Fluid Dynamics*, Cambridge University Press, 2002, ISBN 0-521-59416-2.

[6] C. A. Hirsch, *Numerical Computation of Internal and External Flows*, Wiley and Sons, 1990.

[7] S. Dănăilă, C. Berbente, *Metode numerice în dinamica fluidelor*, Ed. Academiei Române, Bucureşti, 2003.

[8] ***, *Notes on Numerical Fluid Mechanics*, volume 52, Flow Simulation with High-Performance Computers II, Edited by Ernst Heinrich Hirschel, Vieweg 1996.

[9] ***, *Applied Computational Aerodynamics*, vol. 125, Progress in Astronautics and Aeronautics, editor Henne P. A., John Wiley & sons, 1990.

[10] H. F. Creveling, R. H. Carmody, *Axial Flow Compressor Design by Using the Full Radial Equilibrium Theory*, Report NASA-CR–54532, 1986.

[11] ***, *Rotor Dynamic Instability Problems in High Performance Turbomachinery*, Report NASA-CP-2443, Jan. 1987.

[12] I. C. Andrei, About an original method of optimizing the design of axial compressor cascades operating in the stability domain, *INCAS BULLETIN*, (online) ISSN 2247–4528, (print) ISSN 2066–8201, ISSN–L 2066–8201, Volume **5**, Issue 4, DOI: 10.13111/2066-8201.2013.5.4.1, pp. 15-22, 2013.

[13] D. E. Van Zante, A. J. Strazisar, J. R. Wood, M. D. Hathaway, Th. H. Okiishi, Recommendations for Achieving Accurate Numerical Simulation of Tip Clearance Flows in Transonic Compressor Rotors, *ASME Journal of Turbomachinery*, ISSN: 0889-504X, eISSN: 1528-8900, vol. **122**, Issue 4, doi:10.1115/1.1314609, pp. 733-742, October 2000.

[14] D. E. Van Zante, J. J. Adamczyk, A. J. Strazisar, Th. H. Okiishi, Wake recovery Performance Benefit in High Speed Axial Compressor, *ASME Journal of Turbomachinery*, ISSN: 0889-504X, eISSN: 1528-8900, vol. **124**, Issue 2, doi:10.1115/1.1445793, pp. 275-284, April 2002

[15] M. L. Celestina, E. Turkel, *Matrix Viscosity and Preconditioning for Rotating Turbomachinery*, Proceedings of ISROMAC-9, the 9th International Symposium on Transport Phenomena and Dynamics of Rotating Machinery, February 10-1, 2002, Honolulu, Hawaii, USA, 2002-FD-ABS-051.

[16] G. A. Gerolymos, J. Neubauer, V. C. Sharma, I. Vallet, Improved Prediction of Turbomachinery Flows Using Near Wall Reynolds Stress Model, *ASME Journal of Turbomachinery*, ISSN: 0889-504X, eISSN: 1528-8900, vol. **124**, Issue 1, DOI:10.1115/1.1426083, pp. 86-99, Jan. 2002.

[17] M. L. Celestina, J. J. Adamczyk, S. G. Rubin, A Solution Strategy Based on Segmented Domain Decomposition Multigrid for Turbomachinery Flows, *ASME Journal of Turbomachinery*, ISSN: 0889-504X, eISSN: 1528-8900, vol. **124**, Issue 3, doi:10.1115/1.1451085, pp. 341-350, July 2002.

[18] W. Ning, Y. S. Li, R. G. Wells, Predicting Blade Row Interactions Using a Multistage Time-Linearized Navier-Stokes Solver, *ASME Journal of Turbomachinery*, ISSN: 0889-504X, eISSN: 1528-8900, vol. **125**, Issue 1, doi:10.1115/1.1516570, pp. 25-32, January 2003.

[19] L. Sbardella, M. Imregun, Linearized Unsteady Viscous Turbomachinery Flows Using Hybrid Grids, *ASME Journal of Turbomachinery*, ISSN: 0889-504X, eISSN: 1528-8900, vol. **123**, Issue 3, doi:10.1115/1.1371777, pp. 568-582, July 2001.

[20] L. He, T. Chen, R. G. Wells, Y. S. Li, W. Ning, Analysis of Rotor-Rotor and Stator-Stator Interferences in Multi-Stage Turbomachines, *ASME Journal of Turbomachinery*, ISSN: 0889-504X, eISSN: 1528-8900, vol. **124**, Issue 4, doi:10.1115/1.1508382, pp. 564-571, October 2002.

[21] W. S. Clark, K. C. Hall, A Time-Linearized Navier–Stokes Analysis of Stall Flutter, *ASME Journal of Turbomachinery*, ISSN: 0889-504X, eISSN: 1528-8900, vol. **122**, Issue 3, doi:10.1115/1.1303073, pp. 467-476, July 2000.

[22] D. J. Dorney, O. P. Sharma, Evaluation of Flow Field Approximations for Transonic Compressor Stages, *ASME Journal of Turbomachinery*, ISSN: 0889-504X, eISSN: 1528-8900, vol. **119**, Issue 3, doi:10.1115/1.2841143, pp. 445-451, July 1997.

[23] Á. Veress, I. Santa, A 2D mathematical model on transonic axial compressor rotor flow, *Periodica Polytechnica, series of Transportation Engineering*, vol. **30**, nr. 1-2, pp. 53-67, 2002, Budapest University of Technology and Economics, Budapest, 2002.

[24] N. K. Madavan, M. M. Rai, *Computational Analysis of Rotor-Stator Interaction in Turbomachinery Using Zonal Techniques*, cap. 13 in [9]: 481-529, John Wiley & sons, 1990.

[25] I. C. Andrei, N. M. Ene, et al., Topical applications in computational mesh generation from axial compressor to jet engine, *Scientific Bulletin of the "POLITEHNICA" University of Bucharest, Series D: Mechanical Engineering*, volume **67**, no. 2, pp. 101-118, 2005, ISSN 1454-2358, Ed. Politehnica Press, Bucharest, 2005.

[26] I. C. Andrei, *Reseach Report on the Application of Active Disk Theory to a Transonic Highly Loaded Rotor Blade of a Multistaged Axial Flow Compressor*, "POLITEHNICA" University of Bucharest, Faculty of Aerospace Engineering, "Elie Carafoli" Department of Aerospace Sciences, January 2007.

[27] I. C. Andrei, *Studii privind determinarea curgerii prin reţelele de palete de compresor axial destinate motoarelor aeroreactoare*, Referatul 3/ Doctorat /U.P.B., 266 pagini, Bucureşti, 2004.

[28] I. C. Andrei, *Metode Numerice Privind Rezolvarea Ecuaţiilor Diferenţiale ale Dinamicii Gazelor*, Referatul 2/ Doctorat /U.P.B., 100 pagini, Bucureşti, 2003.

[29] I. C. Andrei, *Studii privind compresorul axial*, Referat 1/ Doctorat /U.P.B., 70 pag., Bucureşti, 2002.